A Multi-Source Methodology for Bathymetric Mapping: Integrating In-Situ Measurements with Sentinel-2 Spectral Indices in Mexican Dams

Roberto Ivan Villalobos Martínez [1], Jean Francois Mas [1], Azucena Pérez-Vega [2], Antonio Ruiz Verdú [3], Rosaura Páez Bistrain [1], Luisa Fernanda Chávez Zamora [4], Margarito Álvarez Jara [5], José García Hernández [1], Xavier Sòria-Perpinyà [3], Jesús E. Sáenz-Ceja [6], Jonathan V. Solórzano [1], Melanie Kolb [7], Raúl Aguirre Gómez [7]

[1] CIGA, Universidad Autónoma de México, 58190, Morelia, Michoacán, México - roberto.villalobos.m@hotmail.com, jfmas@ciga.unam.mx, rpaez@ciga.unam.mx, jogarcia@pmip.unam.mx, jsolorzano@ciga.unam.mx
[2] DIGH, University of Guanajuato, Guanajuato, México - azu_pvega@hotmail.com
[3] IPL, University of Valencia, Valencia, España - antonio.ruiz@uv.es, Javier.Soria-Perpina@uv.es
[4] Universidad Michoacana de San Nicolás de Hidalgo, Morelia, Michoacán, México - 2148192a@umich.mx
[5] Universidad Intercultural Indígena de Michoacán, Pátzcuaro, Michoacán - alvarez_jara_m@hotmail.com
[6] IIES, Universidad Autónoma de México, 58190, Morelia, Michoacán, México - jsaenz@cieco.unam.mx
[7] IG, Universidad Nacional Autónoma de México, 04510, Ciudad de México, México - kolb@geografia.unam.mx, raguirre@geografia.unam.mx

Keywords: Bathymetry, remote sensing, USV, in-situ data, water depth estimation, spatio-temporal variability.

Abstract

This study proposes a multi-source methodology for monitoring bathymetry in continental water bodies in central Mexico by integrating in-situ and satellite-based techniques. A 3D-printed Unmanned Surface Vehicle (USV), equipped with echo sounders and GPS, was used to collect high-resolution depth data from five dams: Cointzio and Queréndaro (Michoacán) and Mata, Soledad, and Esperanza (Guanajuato). This data was correlated with Sentinel-2 imagery accessed through the Microsoft Planetary Computer, which provided multispectral, spatio-temporal data across different seasons. To assess water body delineation accuracy, several water indices were compared, including the Normalized Difference Water Index (NDWI), Automated Water Extraction Index with shadows (AWEI_sh), without shadows (AWEI_nsh), Modified NDWI (MNDWI), Sentinel Multi-Band Water Index (SMBWI), and Sentinel-2 Water Index (SWI), along with the Scene Classification Layer (SCL). SWI consistently yielded the most reliable contours. Although the SCL layer struggled in areas with dense aquatic vegetation, misclassifying water surfaces, it proved useful when combined with SWI. This integration produced the most accurate results for most dams— except in Queréndaro, where dense hyacinth cover in parts of the water body and irrigation agriculture in the surroundings impedes the correct detection of water body boundaries. A strong correlation between USV data and satellite-derived contours confirms that combining in-situ and remote sensing sources offers a robust and precise framework for bathymetric mapping in inland waters of Mexico.

1. Introduction

In Mexico, most reservoirs are rain-fed, so they face several problems that reduce reliability and make day-to-day operation harder. Seasonal and uncertain inflows cause large swings in storage—for example, the 210 major dams rose from ~46% to ~72% during the 2025 rainy season—so planning and allocation are difficult (Comisión Nacional del Agua 2025). In warm, dry regions, evaporation is a major loss; reservoirs account for much of global open-water evaporation, and local studies report losses that can take a large share of active storage (Zhao et al. 2022). Sedimentation steadily reduces useful capacity and shortens service life (Gracia 2015). Surface cover also matters: thick mats of invasive water hyacinth hinder operations and water quality, and they can hide open water in optical images, biasing water maps (Rodríguez-Lara et al. 2022). During flood season, multi-purpose reservoirs must balance flood control with saving water under uncertain inflows, which adds stress to rain-dependent systems (Jain et al. 2023); operators may use controlled releases to lower downstream risk—for example, at Cointzio, Michoacán, in October 2025 (Gobierno del Estado de Michoacán 2025). In parallel, rainfall variability undermines freshwater storage and complicates salinity control in rain-fed agro-hydrological systems (Garbanzo, Cameira, and Paredes 2024).

Given these challenges, we need timely and reliable monitoring of reservoirs. In order to accurate and efficient monitoring of continental water bodies is essential for sustainable water resource management, especially in regions affected by seasonal variability and increasing anthropogenic pressures. In order to accurately monitor the water volume in these water bodies, data about the water level and bathymetry must be available. Traditional bathymetric surveys, though precise, are often time-consuming, costly, and limited in spatial and temporal coverage. In recent years, the integration of remote sensing and autonomous platforms has opened new possibilities for enhancing bathymetric mapping, offering scalable and timely solutions for hydrological studies(Kapetanović et al. 2020; Zwolak et al. 2020).

On the other hand, Sentinel-2 imagery, with its high spatial resolution and frequent revisit times, has become a valuable tool for monitoring inland water dynamics. Numerous spectral indices derived from Sentinel-2 data—such as the Normalized Difference Water Index (NDWI), Modified NDWI (MNDWI) (Sekertekin, Cicekli, and Arslan 2018; Vasanthi and Joshitha 2024), and Automated Water Extraction Indices (AWEI)—have been widely used to delineate water bodies. More recent indices like the Sentinel Multi-Band Water Index (SMBWI) and the Sentinel-2 Water Index (SWI) have shown improved accuracy in complex environment. Additionally, the Scene Classification Layer (SCL) provided by the Level-2A Sentinel-2 product offers further potential for land and water discrimination, though its performance varies depending on environmental conditions.

In this study, we present a multi-source methodology that integrates in-situ bathymetric data, collected using a 3D-printed Unmanned Surface Vehicle (USV), with Sentinel-2 satellite

This contribution has been peer-reviewed. The double-blind peer-review was conducted on the basis of the full paper.
https://doi.org/10.5194/isprs-annals-X-3-W3-2025-117-2026

imagery accessed through the Microsoft Planetary Computer. Field measurements were conducted across five dams in central Mexico—Cointzio and Queréndaro in Michoacán, and Mata, Soledad, and Esperanza in Guanajuato. The primary objectives were to evaluate the accuracy of different Sentinel-2 water indices and products (i.e., SCL band) for calculating water extent of different dams, and analysing its correlation with in-situ bathymetry measured by an USV. The findings aim to contribute to the development of a robust and reproducible methodology for bathymetric mapping in inland water bodies across Mexico.

2. Literature Review

Recent research has explored multiple approaches to extracting water bodies from Sentinel-2 imagery, with various spectral indices developed to improve accuracy across diverse landscapes. Among the earliest and most widely used is the Normalized Difference Water Index (NDWI), which has proven effective in several contexts. (Kaplan and Avdan 2017) demonstrated that integrating NDWI with object-based classification methods significantly improved water delineation in mountainous and urban areas. However, subsequent studies have sought to overcome limitations of NDWI in complex environments by developing more robust alternatives.

One such alternative is the Automated Water Extraction Index (AWEI), which includes variants designed to minimize shadow interference. The shadow-free version, AWEI_nsh, has shown superior performance in multiple applications. For instance, it outperformed other indices in identifying inland water bodies in Uganda (Ssekyanzi et al. 2021) and showed high accuracy in delineating the Volta River using Sentinel-2A imagery (Kwang, Osei Jnr, and Amoah 2018). In contrast, AWEI_sh was less effective in both studies. A study in Bath, UK, confirmed these findings, showing that AWEI_nsh produced more accurate predictions than AWEI_sh (Kareem, Attaee, and Omran 2024). Additionally, an AWEI-based method in Google Earth Engine achieved an F1 score of 0.95 in segmenting water bodies from Sentinel and Landsat imagery (Bocchino et al. 2023), further demonstrating its cross-platform reliability.

The Modified NDWI (MNDWI) is another refinement aimed at enhancing water detection, particularly in urban environments. (Du et al. 2016) developed a 10-meter resolution version of MNDWI by sharpening Sentinel-2's SWIR band, resulting in improved detection accuracy. While (Sekertekin et al. 2018) found that NDWI slightly outperformed MNDWI using Sentinel-2 data, (Parihar, Borana, and Yadav 2019) concluded that MNDWI was the most effective among several indices tested, especially when using higher-resolution Sentinel-2A (10 m) imagery compared to 20 m and Landsat 8 OLI (30 m) data.

More recent advancements include the Sentinel Multi-Band Water Index (SMBWI), proposed by (Su et al. 2024). This index incorporates multiple spectral bands from Sentinel-2 to effectively suppress interference from vegetation, clouds, buildings, and complex terrain. The SMBWI achieved a total classification accuracy exceeding 96.5% and had the lowest total error among nine water indices. It was particularly effective in identifying mixed water and non-water pixels, making it one of the most robust tools for large-scale surface water mapping.

In parallel, the Sentinel-2 Water Index (SWI) was introduced by (Jiang et al. 2020, 2021), who utilized red-edge and shortwave infrared bands to improve water detection across various environments. The integration of SWI with the Otsu thresholding algorithm further enhanced its effectiveness in suppressing shadows in urban areas. Compared to traditional indices like NDWI, SWI demonstrated consistently superior performance, making it highly suitable for diverse hydrological applications.

Complementing spectral indices, the Scene Classification Layer (SCL) provided by the Sen2Cor Level-2A processor classifies pixels into land cover types using a combination of visual inspection, cross-sensor comparison, and meteorological data (Main-Knorn et al. 2017). While the SCL is useful in many applications, it faces limitations in areas with dense aquatic vegetation, where it may misclassify water surfaces. Nevertheless, when used in conjunction with spectral indices like SWI, the SCL can enhance overall delineation accuracy.

Recent research has also focused on developing unmanned surface vehicles (USVs) for bathymetric surveys, offering advantages over traditional methods. These autonomous platforms integrate various sensors, such as echosounders and environmental monitors, to collect high-resolution depth data (Maulana et al. 2024; Sotelo-Torres, Alvarez, and Roberts 2023). When deployed in situ, USVs can serve as a valuable complement to satellite-based methods by providing ground-truth data that enhances the accuracy of remote sensing analyses. By correlating USV-derived measurements with water body contours obtained through spectral indices—such as NDWI, MNDWI, SWI, or SMBWI—it becomes possible to account for seasonal hydrological dynamics that influence dam volume and surface extent. This integration allows for a more nuanced and temporally responsive bathymetric mapping approach. While USVs may face limitations in certain environments, their ability to validate and refine satellite-derived estimations makes them an essential tool for achieving higher precision in bathymetric measurements.

Collectively, these studies demonstrate that integrating traditional and advanced spectral indices with scene classification products provides a more comprehensive and accurate approach for water body extraction using Sentinel-2 data, especially when complemented by bathymetric measurements obtained via echosounders mounted on unmanned surface vehicles (USVs).

3. Methodology

This study employed a multi-source methodological framework combining in-situ bathymetric measurements and satellite remote sensing data to analyze inland water bodies in central Mexico. Five dams were selected as case studies: Cointzio and Queréndaro in Michoacán, Soledad, Esperanza, and Mata in Guanajuato. These sites were chosen based on accessibility, variability in size, vegetation cover, and seasonal water dynamics.

3.1 Study Sites and Reservoir Characteristics

The Cointzio Dam (Fig. 1a), located near Morelia, Michoacán, México (coordinates: 19°37′48.50″ N, 101°15′32.40″ W), has a storage capacity of 68.520 hm³. The Queréndaro Dam (Fig. 1b), also situated near Morelia (coordinates: 19°49′01″ N, 100°52′15″ W), has an estimated capacity of 1.9 hm³ and primarily serves irrigation and agricultural purposes.

The Soledad Dam (Fig. 1c), located in Guanajuato, México (coordinates: 21°02′25″ N, 101°16′48″ W), has an estimated

storage capacity of approximately 5.1 hm³ and is mainly used for local water supply.

The La Esperanza Dam, situated just north of Guanajuato City in the Bajío region (coordinates: 21°03′00″ N, 101°15′22″ W; approx. 21.05004° N, 101.25596° W), municipal water. According to CONAGUA's 2021 data, it has a maximum capacity of about 4.0 hm³, with typical storage levels near that amount. More recent reports indicate that it has occasionally reached full capacity (3.92 hm³).

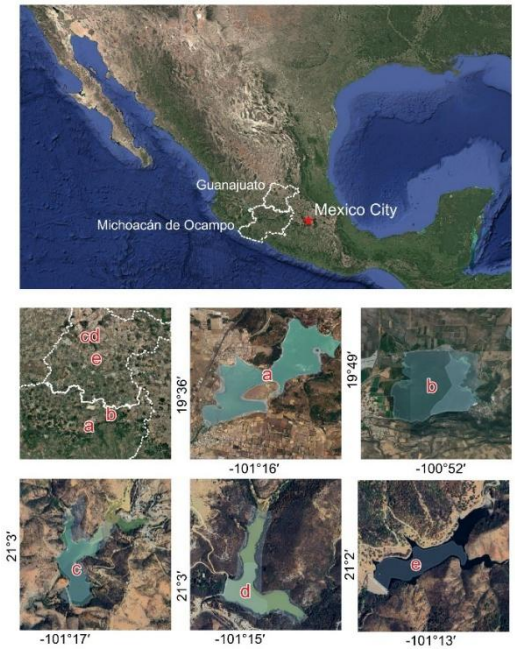

Figure 1. Geographic Location of the Studied Dams in Central Mexico: Cointzio a), Queréndaro b) (Michoacán), and Soledad c), Esperanza d) and Mata e) (Guanajuato).

The Mata Dam, located east of Guanajuato City within the same municipality (approximate coordinates: 21°01′36″ N, 101°13′18″ W, or 21.0266° N, –101.2217° W), has a capacity of 0.015 hm³. Like the other dams, it primarily serves water supply needs, fulfilling a similar role to other small- and medium-sized reservoirs in the region.

3.2 In-Situ Data Collection

Bathymetric data were collected using a custom-built, 3D-printed Unmanned Surface Vehicle (USV), equipped with a single-beam echosounder and high-precision GPS (Fig 2).

Figure 2. Uncrewed Surface Vehicle (USV) developed in-house for inland water monitoring and bathymetric surveying.

The USV, controlled via remote control, was deployed across each dam to systematically capture water depth at consistent spatial intervals. The collected data—including bathymetry, temperature, and GPS coordinates—were post-processed to eliminate noise and inconsistencies, particularly from incomplete or null values.

The USV measures 1.00 m × 1.00 m × 0.55 m and was 3D-printed using ABS, a material chosen for its enhanced resistance to environmental conditions. Designed for inland water applications, the USV demonstrated high stability during field testing, withstanding wind speeds of up to 20 km/h and wave heights of up to 30 cm—making it the most stable platform developed by our team to date. It features a communication system with a maximum operational range of 550 meters, and it is currently the active prototype used in all field deployments.

The datasets generated and/or analyzed during the current study are available upon reasonable request. Access can be obtained via the following Google Drive link: https://drive.google.com/drive/folders/1DjGrIjn5rm1eD6aTlMqrkkeIhM5--q5s?hl=es. Alternatively, interested researchers may contact the corresponding author at roberto.villalobos.m@hotmail.com for further information

3.3 Satellite data acquisition

Sentinel-2 Level-2A imagery was accessed through Microsoft's Planetary Computer platform, covering a temporal range from January 1, 2023, to May 30, 2025. A circular area of interest was defined based on geographic coordinates, and imagery was filtered by tile ID, acquisition date, and cloud cover percentage, with a maximum cloud cover threshold of 10% applied to ensure image quality. The STAC API was queried to retrieve matching image metadata, and relevant spectral bands—such as B01 (coastal), B02 (blue), B03 (green), B04 (red), B08 (NIR), B10 (cirrus), B11 (SWIR1), and B12 (SWIR2)—were selected for download. The selected imagery was then clipped to the defined region of interest and saved as GeoTIFF files for further analysis. This process was automated and parallelized using Python to improve download and processing efficiency.

3.4 Water Index Calculation and Contour Extraction

NDWI, AWEI (shadow and non-shadow variants), MNDWI, MBWI, and SWI—were computed after reprojecting and resampling required bands to a common spatial resolution.

The Normalized Difference Water Index (NDWI) is designed to enhance water features while suppressing vegetation and soil:

$$NDWI = \frac{Green - NIR}{Green + NIR} = \frac{B_{03} - B_{08}}{B_{03} + B_{08}} \quad (1)$$

The Modified NDWI (MNDWI) improves water detection in urban or built-up areas:

$$MNDWI = \frac{Green - SWIR1}{Green + SWIR1} = \frac{B_{03} - B_{11}}{B_{03} + B_{11}} \quad (2)$$

The Automated Water Extraction Index - Non-Shadow (AWEI_nsh) enhances separation between water and built-up areas:

$$AWEI_{nsh} = B_{01} + 2.5 * B_{02} - 1.5 * (B_{04} + B_{05}) - 0.25 * B_{08} \quad (3)$$

The Automated Water Extraction Index - Shadow (AWEI_sh) is designed to detect water in shaded or clouded regions:

$$AWEI_{sh} = B_{01} + 2.5 * B_{02} - 1.5 * (B_{04} + B_{05}) - 0.25 * B_{08} - 1.5 \quad (4)$$

The Modified Bare Water Index (MBWI) distinguishes between bare land and water using a combination of spectral bands:

$$MBWI = \frac{B_{03}+B_{11}-B_{08}-B_{05}}{B_{03}+B_{11}+B_{08}+B_{05}} \quad (5)$$

The Shadow Water Index (SWI) is an empirical index combining blue, green, and SWIR bands to detect water even under low illumination:

$$SWI = (B_{03} - B_{08}) * (\frac{B_{01}}{B_{05}}) \quad (6)$$

Threshold-based masking and connected component analysis were applied to each index to identify water bodies and estimate their surface area in square kilometers. At each date, spectral index values near the reference point were extracted, and RGB composites, water masks, and contour visualizations were generated for spatial context. Results were saved as GeoTIFFs and summarized in multi-panel figures.

Complementing this, a class-based Python pipeline (WaterBodyAnalyzer) was used to analyze binary water masks derived from the satellite data. It filters scenes based on surface area thresholds and changes in water extent over time (delta_area), visualizes the results with respect to in-situ depth measurements, and exports both pixel-level water locations and contour boundaries in geographic coordinates. This integrated remote sensing and geospatial analysis enables a detailed, time-resolved understanding of water surface dynamics at the study site

Additionally, the Scene Classification Layer (SCL) from Sentinel-2 was used to enhance water detection by masking out vegetation, clouds, and land pixels. Water body contours were extracted for each index using adaptive thresholding and refined using morphological operations.

3.5 Correlation and Validation

Water contours derived from each index were visually compared against the bathymetric data collected by the USV. Metrics such as area overlap, shoreline displacement, and water area differences were calculated. Special attention was given to the integration of SWI and SCL, which yielded the most reliable results for most dams. However, dense water hyacinth caused the method to underestimate water extent by shrinking the mapped open-water polygon, even though water is present beneath the vegetation. In contrast, recently irrigated fields beside the dam led the method to overestimate the water outline because the SWI responds to surface moisture.

4. Results

A multi-temporal panel (Figure 3) was constructed to visually compare the performance of six water-related spectral indices—NDWI, AWEI_sh, AWEI_nsh, MNDWI, MBWI, and SWI—and the SCL layer of Sentinel 2 across multiple dates at the Cointzio Dam. Each row corresponds to a different acquisition date, while each column depicts either the RGB image, one of the spectral indices, or classification layers. The visual comparison reveals distinct behaviors:

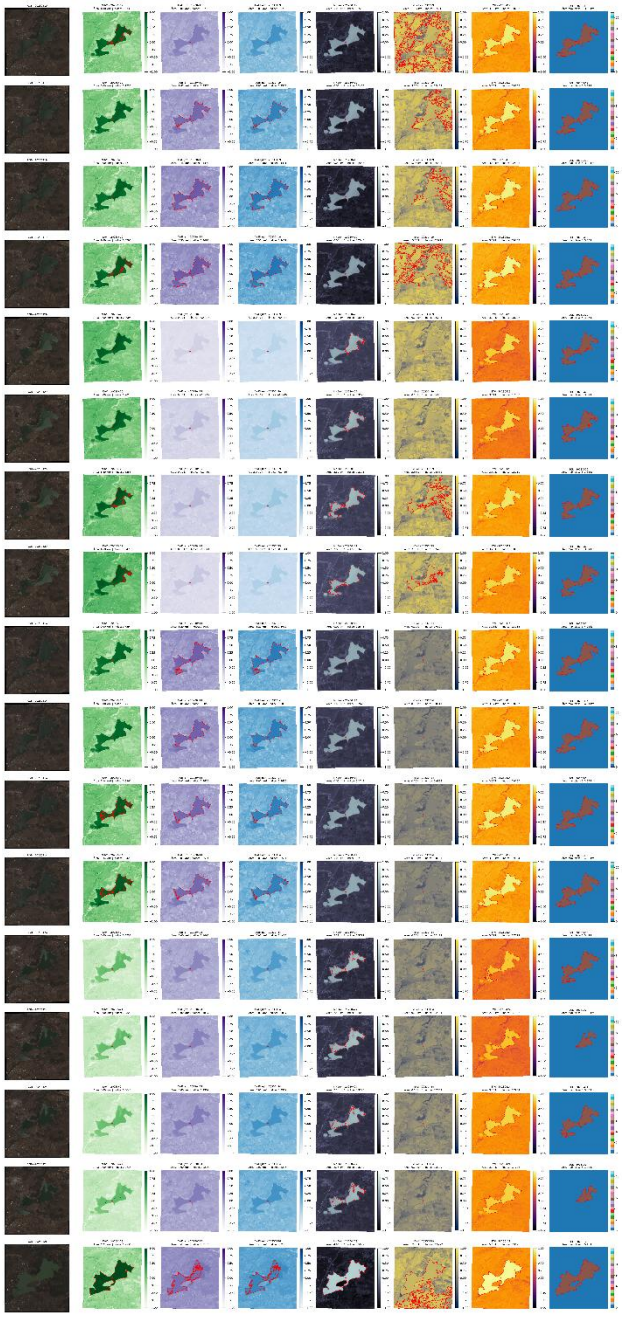

Figure 3. Visual comparison of RGB imagery, spectral water indices (NDWI, AWEI, AWEI, MNDWI, MBWI, SWI), and the Scene Classification Layer (SCL) from Sentinel-2, including derived water contours.

- NDWI and MNDWI yielded the poorest results in delineating water boundaries. In several instances, they failed to detect any water body at all, primarily due to the dense presence of floating vegetation, particularly water lilies, which significantly distorted the spectral response.
- AWEI_sh and AWEI_nsh, designed to enhance water detection in shadowed environments, exhibited

high sensitivity. However, they also introduced substantial noise by misclassifying areas with high total dissolved solids (TDS) and total suspended solids (TSS) as land, thus reducing their reliability in turbid conditions.

- MBWI, overestimate all the terrain in all cases making impossible to identify the water body.
- SWI (Shallow Water Index) exhibited the most stable performance of the indexes analyzed, maintaining clear water delineation even under adverse conditions such as cloud contamination, presence of superficial vegetation (lily) or variable water turbidity.
- SCL (Scene Classification Layer) demonstrated high accuracy and consistent performance in most cases. However, its effectiveness decreased in scenarios with extremely dense surface vegetation, where water detection was significantly hindered.

The integration of SCL and SWI offered several key advantages:

- Noise Reduction: SCL effectively masked water coverage in most of the cases, reducing spectral confusion and false positives from SWI in non-water areas.
- Improved Boundary Accuracy: SCL provided categorical pixel labeling, while SWI contributed gradient-based detection. Their combination preserved the sharp boundaries of water bodies while minimizing misclassification.
- Turbidity Resilience: SCL occasionally misclassified turbid water as land or vegetation. SWI, being a continuous index, retained sensitivity to these conditions, allowing better representation of water extent.
- Consistency Over Time: Across all observed dates, the SWI+SCL combination maintained the highest consistency in delineating the true water extent, regardless of seasonality or atmospheric conditions.

Figure 4 displays the spatial and temporal variation of water surface extent for Cointzio dam, derived from Sentinel-2 imagery over multiple acquisition dates. The water contours were generated using the combined Shallow Water Index (SWI) and Scene Classification Layer (SCL class 6: water), ensuring enhanced accuracy and minimal interference from clouds, shadows, and land features.

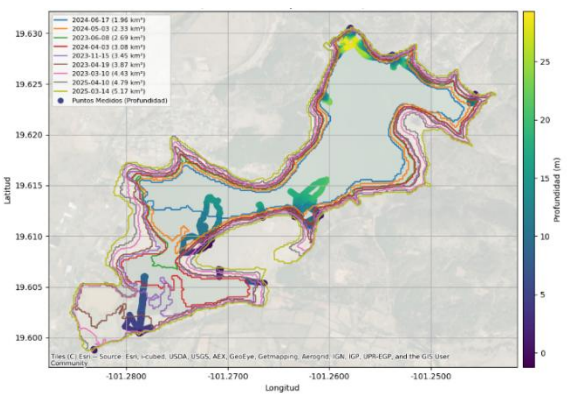

Figure 4. Correlation between in-situ bathymetric data collected via USV and water contours derived from nine Sentinel-2 images between March 2023 and April 2025 at Cointzio Dam.

The extracted water contours from nine dates between March 2023 and April 2025 are overlaid on the base map, along with in-situ bathymetric measurement points. Each contour is color-coded by area maximum surface extent from 5.17km^2 in March 2025 to a minimum of 1.96km^2 in March 2023, indicating substantial surface loss over the dry period.

The strong correlation between the spectral contours and bathymetric depth supports the reliability of using Sentinel-2 SWI+SCL masks for temporal surface water monitoring in dam systems.

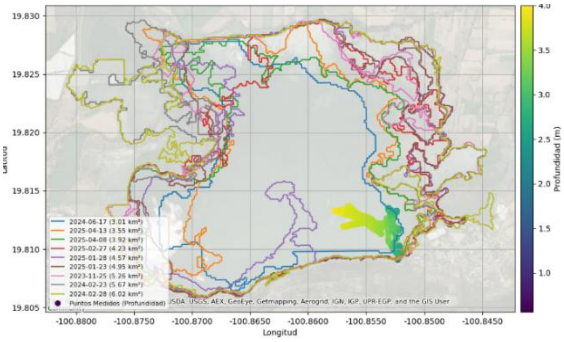

Figure 5. Correlation between in-situ bathymetric data collected via USV and water contours derived from nine Sentinel-2 images between November 2023 and April 2025 at Queréndaro Dam.

The same processing workflow applied in Figures 5 through 8 produced markedly different outcomes at each site. In the case of Queréndaro Dam, the automated water-contour extraction was frequently misled by the surrounding irrigated croplands. High soil moisture in these agricultural areas caused the SWI to overestimate water extent, classifying recently watered fields as part of the reservoir. Compounding this problem, Queréndaro is exceptionally shallow—no more than 4 m at its deepest point—and contains the densest cover of surface vegetation among all reservoirs examined. These two factors severely limited the ability of a satellite-only approach to generate accurate water boundaries for this site.

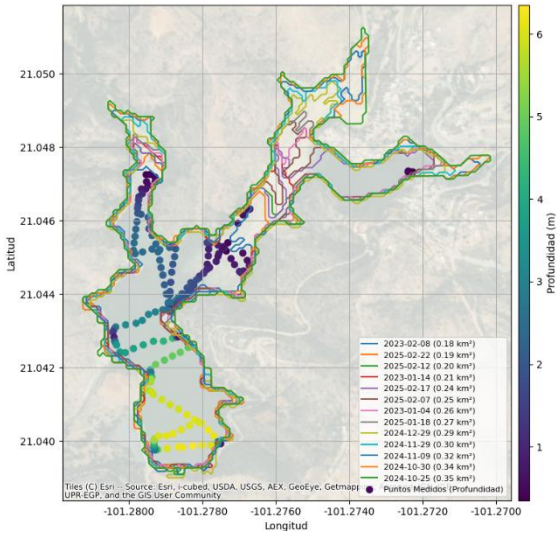

Figure 6. Correlation between in-situ bathymetric data collected via USV and water contours derived from nine Sentinel-2 images between January 2023 and April 2025 at Soledad Dam.

The correlation at Soledad Dam (Figure 6) showed high precision, particularly for the water contours derived from SCL and SWI. This accuracy can be attributed to the absence of surrounding agricultural fields and the clearly defined boundaries of the reservoir, which are reinforced by built infrastructure. In this case, the northeastern region of the dam was identified as the shallowest area. However, it was not possible to collect bathymetric data there during fieldwork, as the region was completely dry at the time of the visit.

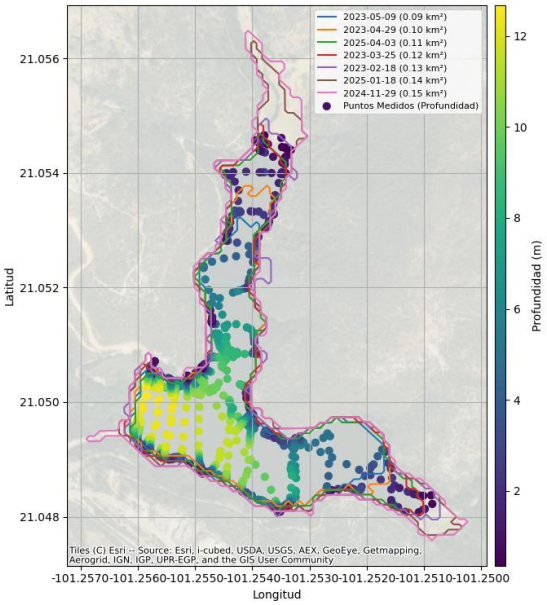

Figure 7. Correlation between in-situ bathymetric data collected via USV and water contours derived from nine Sentinel-2 images between February 2023 and April 2025 at Esperanza Dam.

At Esperanza Dam (figure 7), we were able to collect a larger volume of in-situ bathymetric data due to the dam's size and the fact that it was nearly at full capacity during the field survey. Satellite imagery revealed that the shallowest zones are located along the northern and eastern branches of the reservoir, with depths ranging from 0 to 12.4 meters. It is worth noting that some of the water contours slightly overestimated the water extent, particularly near the dam curtain, where delineation was less precise.

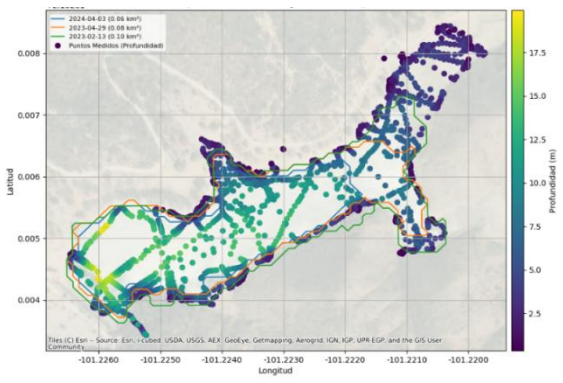

Figure 8. Correlation between in-situ bathymetric data collected via USV and water contours derived from nine Sentinel-2 images between February 2023 and April 2024 at Mata Dam.

At Mata Dam, we observed the opposite situation compared to Esperanza. In this case, the water contours derived from satellite imagery underestimated the actual water extent. As shown in Figure 8, we collected in-situ bathymetric data in areas—particularly in the northeast—where no satellite-derived contours were detected. This discrepancy may be due to the limited range of acquisition dates or the interference from mountain shadows surrounding the dam, which likely affected the accuracy of the water delineation.

5. Discussion

The multi-temporal experiment confirms that index choice and ancillary masks are decisive when reservoirs are small, shallow, vegetated, or turbid:

- Index behavior – NDWI, MNDWI, and MBWI all broke down under the extreme optical complexity of Cointzio, routinely missing water or flooding the entire scene. AWEI variants, though more sensitive, remained vulnerable to high TDS/TSS levels and therefore produced noisy, fragmented masks. In contrast, SWI preserved a coherent water signal across vegetation, clouds, and turbidity, validating its design for mixed pixels. However, these results also highlight the importance of experimenting with different threshold values (umbral settings) for each index, as fixed, global thresholds may not be optimal across all environmental conditions. To enhance accuracy, it is essential to calibrate these thresholds not only using data from Cointzio but also from other reservoirs with contrasting characteristics. For example, in Queréndaro dam, dense mats of water hyacinth contracted the mapped open-water polygon, underestimating water extent even where water exists under the vegetation. In contrast, recently irrigated fields adjacent to the dam overestimated the water outline due to the SWI's sensitivity to surface moisture. Including such diverse cases in the calibration process can help develop more robust and adaptive threshold criteria for different hydro-environmental contexts.
- Ancillary information – The categorical Scene Classification Layer (SCL) supplied a valuable, physically independent constraint. When SWI was multiplied with SCL class 6, most land- and cloud-related false positives disappeared, while SWI's continuous nature recovered water that SCL alone mis-classed as land during very turbid episodes.
- Spatial generalisation limits – Transferring the SWI + SCL workflow to the four additional dams exposed context-specific weaknesses.
    - Queréndaro: irrigated cropland moisture and ultra-shallow depths (< 4 m) mimicked open water in SWI; disrupted the optical signal.
    - Soledad: clear margins and cero agriculture yielded excellent agreement between satellite–derived and in-situ contours, emphasizing that structural embankments simplify classification.

https://doi.org/10.5194/isprs-annals-X-3-W3-2025-117-2026

- Esperanza: high water levels allowed extensive bathymetry, showing good depth–contour correspondence yet slight over-delineation near the curtain, possibly from sunglint or steep walls.
- Mata: mountain shadows and the limited temporal stack led SWI + SCL to miss water in the northeastern embayment, revealing that topographic shading and temporal gaps are the dominant error sources when turbidity are moderate.

Collectively these findings support the SWI + SCL fusion as the most portable solution among the tested optical options, but also highlight the site-specific error modes that remain when only multispectral data are used.

6. Conclusions

This methodological integration allowed for a robust evaluation of spectral indices in varying seasonal and ecological conditions, supporting the development of a reliable workflow for bathymetric mapping in Mexican inland waters.

Robust delineation with SWI + SCL – Across 28 months (March 2023 – April 2025) at Cointzio, the fusion approach captured seasonal shoreline migration from 1.96 km² (March 2023) to 5.17 km² (March 2025) while suppressing ~90 % of the false positives observed in single-index masks.

Bathymetric consistency – The tight spatial correspondence between satellite contours and echo-sounder depths at three of the five dams demonstrates that Sentinel-2 can serve as a low-cost proxy for monthly to seasonal surface-area monitoring, even where detailed sonar surveys are sporadic.

Contextual limitations – Performance degrades in reservoirs that are (i) extremely shallow with floating vegetation, (ii) bordered by irrigated fields, or (iii) surrounded by steep terrain casting persistent shadows. These contexts demand additional data streams.

In summary, the optical-only workflow is ready for routine operational monitoring in clear-margin, medium-depth dams, but remains insufficient for the most challenging optical scenes.

7. Future work

SAR–Optical fusion – Incorporate Sentinel-1 backscatter to discriminate water in vegetated or turbid conditions where optical indices saturate.

Adaptive, site-specific thresholds – Replace a global SWI cut-off with a machine-learning model (e.g., Random Forest or U-Net) that ingests SWI, spectral bands and terrain–derived variables, trained on limited field masks to adapt to local superficial vegetation and turbidity regimes.

High-resolution constellations – Test PlanetScope or SkySat imagery to resolve narrow irrigation canals and vegetated patches that confuse 10 m pixels at Queréndaro.

LiDAR or UAV bathymetry validation – Acquire shallow-water LiDAR or drone photogrammetry to ground-truth depth in ultra-shallow areas where sonar boats cannot navigate, refining area–volume curves.

Operational dashboard – Embed the workflow in a cloud platform (e.g., Microsoft Planetary) with automatic alerting when area drops below management thresholds, delivering real-time intelligence to reservoir operators.

Executing these steps will push the methodology from a research prototype to a robust, region-wide decision support system for reservoir management under increasing hydrological stress.

Acknowledgements

We sincerely appreciate the support of the project *"Azolvamiento y eutrofización en presas periurbanas de zonas templadas de México"*, funded under the *Programa de Apoyo a Proyectos de Investigación e Innovación Tecnológica* (PAPIIT), clave IN112823. This research would not have been possible without their support

This paper was wrote using AI-assited tools for grammatical correction and language refinement during the preparation.

References

Bocchino, F., R. Ravanelli, V. Belloni, P. Mazzucchelli, and M. Crespi. 2023. "Water Reservoirs Monitoring through Google Earth Engine: Application to Sentinel and Landsat Imagery." *International Archives of the Photogrammetry, Remote Sensing and Spatial Information Sciences - ISPRS Archives* 48(M-1–2023):41–47. doi:10.5194/ISPRS-ARCHIVES-XLVIII-M-1-2023-41-2023,.

Comisión Nacional del Agua. 2025. "Presas de México Alcanzan El 72 % de Llenado Durante La Temporada de Lluvias 2025 | Comisión Nacional Del Agua | Gobierno | Gob.Mx." https://www.gob.mx/conagua/prensa/presas-de-mexico-alcanzan-el-72-de-llenado-durante-la-temporada-de-lluvias-2025.

Du, Yun, Yihang Zhang, Feng Ling, Qunming Wang, Wenbo Li, and Xiaodong Li. 2016. "Water Bodies' Mapping from Sentinel-2 Imagery with Modified Normalized Difference Water Index at 10-m Spatial Resolution Produced by Sharpening the SWIR Band." *Remote Sensing 2016, Vol. 8, Page 354* 8(4):354. doi:10.3390/RS8040354.

Garbanzo, Gabriel, Maria do Rosário Cameira, and Paula Paredes. 2024. "The Mangrove Swamp Rice Production System of Guinea Bissau: Identification of the Main Constraints Associated with Soil Salinity and Rainfall Variability." *Agronomy 2024, Vol. 14, Page 468* 14(3):468. doi:10.3390/AGRONOMY14030468.

Gobierno del Estado de Michoacán. 2025. "Mantiene Gobierno de Michoacán Operativo de Vigilancia Ante Desfogue Controlado de La Presa de Cointzio." https://www.gob.mx/conagua/prensa/presas-de-mexico-alcanzan-el-72-de-llenado-durante-la-temporada-de-lluvias-2025.

Gracia, Jesús. 2015. "La Sedimentación, Suelo Útil Que Inutiliza Presas En México." https://www.dgcs.unam.mx/boletin/bdboletin/2015_444.html.

Jain, Sharad K., L. S. Shilpa, Deepti Rani, and K. P. Sudheer. 2023. "State-of-the-Art Review: Operation of Multi-Purpose Reservoirs during Flood Season." *Journal of Hydrology* 618:129165. doi:10.1016/J.JHYDROL.2023.129165.

Jiang, W., Y. Ni, Z. Pang, G. He, J. Fu, J. Lu, K. Yang, T. Long, and T. Lei. 2020. "A New Index for Identifying Water Body from Sentinel-2 Satellite Remote Sensing Imagery." *ISPRS Annals of the Photogrammetry, Remote Sensing and Spatial Information Sciences* V-3–2020:33–38. doi:10.5194/ISPRS-ANNALS-V-3-2020-33-2020,.

Jiang, Wei, Yuan Ni, Zhiguo Pang, Xiaotao Li, Hongrun Ju, Guojin He, Juan Lv, Kun Yang, June Fu, and Xiangdong Qin. 2021. "An Effective Water Body Extraction Method with New Water Index for Sentinel-2 Imagery." *Water 2021, Vol. 13, Page 1647* 13(12):1647. doi:10.3390/W13121647.

Kapetanović, Nadir, Antonio Vasilijević, Đula Nađ, Krunoslav Zubčić, and Nikola Mišković. 2020. "Marine Robots Mapping the Present and the Past: Unraveling the Secrets of the Deep." *Remote Sensing 2020, Vol. 12, Page 3902* 12(23):3902. doi:10.3390/RS12233902.

Kaplan, Gordana, and Ugur Avdan. 2017. "Object-Based Water Body Extraction Model Using Sentinel-2 Satellite Imagery." *European Journal of Remote Sensing* 50(1):137–43. doi:10.1080/22797254.2017.1297540.

Kareem, Hayder H., Muammar H. Attaee, and Zainab Ali Omran. 2024. "Estimation of the Water Ratio Index (WRI) and Automated Water Extraction Index (AWEI) of Bath in the United Kingdom Using Remote Sensing Technology of the Multispectral Data of Landsat 8-OLI." *Water Conservation & Management* 8(2):171–78. doi:10.26480/WCM.02.2024.171.178.

Kwang, Clement, Edward Matthew Osei Jnr, and Adwoa Sarpong Amoah. 2018. "Comparing of Landsat 8 and Sentinel 2A Using Water Extraction Indexes over Volta River." *Journal of Geography and Geology* 10(1):1–7. doi:10.5539/JGG.V10N1P1.

Main-Knorn, Magdalena, Bringfried Pflug, Jerome Louis, Vincent Debaecker, Uwe Müller-Wilm, and Ferran Gascon. 2017. "Sen2Cor for Sentinel-2." *In Image and Signal Processing for Remote Sensing XXIII (Proc. SPIE Vol. 10427, 1042704). SPIE.* doi:10.1117/12.2278218.

Maulana, Adam, Joko Endrasmono, Zindhu Maulana, Ahmad Putra, Lilik Subiyanto, Mohammad Basuki Rahmat, M. Khoirul Hasin, Isa Rachman, Agus Khumaidi, Yuning Widiarti, Ryan Yudha Adhitya, and Pristovani Riananda. 2024. "Accessing Ping Sonar Echosounder Produksi ROVMAKER Pada Mikrokontroler Dan Data Noise Reduction Dengan Kalman Filter." *Jurnal Elektronika Dan Otomasi Industri* 11(1):274–86. doi:10.33795/ELKOLIND.V11I1.5389.

Parihar, S. K., S. L. Borana, and S. K. Yadav. 2019. "Comparative Evaluation of Spectral Indices and Sensors for Mapping of Urban Surface Water Bodies in Jodhpur Area : Smart Sustainable Growth." *Proceedings - 2019 International Conference on Computing, Communication, and Intelligent Systems, ICCCIS 2019* 2019-January:484–89. doi:10.1109/ICCCIS48478.2019.8974505.

Rodríguez-Lara, Jessica W., Francisco Cervantes-Ortiz, Gerónimo Arámbula-Villa, and Luis A. Mariscal-Amaro. 2022. "Lirio Acuático (Eichhornia Crassipes): Una Revisión." *Agronomía Mesoamericana* e44201:33. doi:10.15517/am.v33i1.44201.

Sekertekin, Aliihsan, Sevim Yasemin Cicekli, and Niyazi Arslan. 2018. "Index-Based Identification of Surface Water Resources Using Sentinel-2 Satellite Imagery." *ISMSIT 2018 - 2nd International Symposium on Multidisciplinary Studies and Innovative Technologies, Proceedings*. doi:10.1109/ISMSIT.2018.8567062.

Sotelo-Torres, Fernando, Laura V. Alvarez, and Robert C. Roberts. 2023. "An Unmanned Surface Vehicle (USV): Development of an Autonomous Boat with a Sensor Integration System for Bathymetric Surveys." *Sensors 2023, Vol. 23, Page 4420* 23(9):4420. doi:10.3390/S23094420.

Ssekyanzi, Athanasius, Nancy Nevejan, Dimitry Van der
Zande, Molly E. Brown, and Gilbert Van Stappen. 2021.
"Identification of Potential Surface Water Resources for Inland Aquaculture from Sentinel-2 Images of the Rwenzori Region of Uganda." *Water* 13(19):2657. doi:10.3390/W13192657.

Su, Zhenfeng, Longwei Xiang, Holger Steffen, Lulu Jia, Fan Deng, Wenliang Wang, Keyu Hu, Jingjing Guo, Aile Nong, Haifu Cui, and Peng Gao. 2024. "A New and Robust Index for Water Body Extraction from Sentinel-2 Imagery." *Remote Sensing 2024, Vol. 16, Page 2749* 16(15):2749. doi:10.3390/RS16152749.

Vasanthi, A., and K. Lakshmi Joshitha. 2024. "Water Body Detection Utilizing NDWI, NDVI and NMDWI Indices in SEN-12 Spectral Imagery." *Proceedings - 1st International Conference on Electronics, Communication and Signal Processing, ICECSP 2024*. doi:10.1109/ICECSP61809.2024.10698263.

Zhao, Gang, Yao Li, Liming Zhou, and Huilin Gao. 2022. "Evaporative Water Loss of 1.42

Million Global Lakes." *Nature Communications* 13(1), 3686. doi:10.1038/s41467-022-31125-6.

Zwolak, Karolina, Rochelle Wigley, Aileen Bohan, Yulia Zarayskaya, Evgenia Bazhenova, Wetherbee Dorshow, Masanao Sumiyoshi, Seeboruth Sattiabaruth, Jaya Roperez, Alison Proctor, Craig Wallace, Hadar Sade, Tomer Ketter, Benjamin Simpson, Neil Tinmouth, Robin Falconer, Ivan Ryzhov, and Mohamed Elsaied Abou-Mahmoud. 2020. "The Autonomous Underwater Vehicle Integrated with the Unmanned Surface Vessel Mapping the Southern Ionian Sea. The Winning Technology Solution of the Shell Ocean Discovery XPRIZE." *Remote Sensing 2020, Vol. 12, Page 1344* 12(8):1344. doi:10.3390/RS12081344.